



Published in final edited form as:

J Invest Surg. 2008 ; 21(3): 101–108. doi:10.1080/08941930802043565.

Altered Expression of Zonula Occludens-2 Precedes Increased Blood-Brain Barrier Permeability in a Murine Model of Fulminant Hepatic Failure

Naoki Shimojima,

Department of Transplantation, Division of Transplant Surgery, Mayo Clinic College of Medicine, Jacksonville, Florida

Christopher B. Eckman,

Department of Neuroscience, Mayo Clinic College of Medicine, Jacksonville, Florida

Michael McKinney,

Department of Neuroscience, Mayo Clinic College of Medicine, Jacksonville, Florida

Daniel Sevelev,

Department of Neuroscience, Mayo Clinic College of Medicine, Jacksonville, Florida

Satoshi Yamamoto,

Department of Transplantation, Division of Transplant Surgery, Mayo Clinic College of Medicine, Jacksonville, Florida

Wenlang Lin,

Department of Neuroscience, Mayo Clinic College of Medicine, Jacksonville, Florida

Dennis W. Dickson, and

Department of Neuroscience, Mayo Clinic College of Medicine, Jacksonville, Florida

Justin H. Nguyen

Department of Transplantation, Division of Transplant Surgery, Mayo Clinic College of Medicine, Jacksonville, Florida

Abstract

Brain edema secondary to increased blood-brain barrier (BBB) permeability is a lethal complication in fulminant hepatic failure (FHF). Intact tight junctions (TJ) between brain capillary endothelial cells are critical for normal BBB function. However, the role of TJ in FHF has not been explored. We hypothesized that alterations in the composition of TJ proteins would result in increased BBB permeability in FHF. In this study, FHF was induced in C57BL/6J mice by using azoxymethane. BBB permeability was assessed with sodium fluorescein. Expression of TJ proteins was determined by Western blot, and their cellular distribution was examined using immunofluorescent microscopy. Comatose FHF mice had significant cerebral sodium fluorescein extravasation compared with control and precoma FHF mice, indicating increased BBB permeability. Western blot analysis showed a significant decrease in zonula occludens (ZO)-2 expression starting in the precoma stage. Immunofluorescent microscopy showed a significantly altered distribution pattern of ZO-2 in

Address correspondence to Justin H. Nguyen, Division of Transplant Surgery, Mayo Clinic College of Medicine, 4205 Belfort Road, Suite 1100, Jacksonville, Florida 32216. E-mail: nguyen.justin@mayo.edu.

Naoki Shimojima is now at Keio University School of Medicine, Department of Surgery, 35 Shinanomachi Shinjuku-ku, Tokyo, 160-8582, Japan.

Satoshi Yamamoto is now at Division of Digestive and General Surgery, Niigata University Graduate School of Medical and Dental Sciences, Asahimachi-dori 1-757, Niigata 951-8510, Japan.

isolated microvessels from precoma FHF mice. These changes were more prominent in comatose FHF animals. Significant alterations in ZO-2 expression and distribution in the tight junctions preceded the increased BBB permeability in FHF mice. These results suggest that ZO-2 may play an important role in the pathogenesis of brain edema in FHF.

Keywords

tight junction; ZO-2; blood-brain barrier permeability; brain edema; acute liver failure

Fulminant hepatic failure (FHF) is a clinical syndrome associated with massive hepatocellular necrosis and severe liver dysfunction in the absence of previous liver disease. Patients in early stages of FHF may recover spontaneously. However, during stages III and IV (comatose stages), when encephalopathy and brain edema occur, the disease takes a rapidly progressive and lethal course [1-3]. Brain edema in FHF results from compromised blood-brain barrier (BBB) permeability, leading to increased extravasation of water and other small molecules into the brain [2,3].

The tight junction (TJ) complex between endothelial cells in the BBB consists of proteins such as occludin, claudins, junctional adhesion molecules, and zonula occludens (ZO) [4]. An intact TJ is required to maintain normal BBB function. Altered TJ proteins have been associated with increased BBB permeability in various pathologic conditions in the brain. For instance, occludin and ZO-1 are implicated in BBB dysfunction in ischemic brain injury [5,6]. Selective loss of claudin-3 with resulting brain edema occurs in autoimmune encephalitis and glioblastoma multiforme [7,8]. Gene deletion of claudin-5 is associated with altered permeability in which only small molecules may cross the BBB [9].

To date, there are limited data on changes in the composition of brain endothelial cells in FHF. Certain astrocyte genes have been shown to be significantly altered in FHF [10]. Both endothelial and astrocytic glucose transporter proteins are selectively altered in brains of FHF animals [11]. However, the role of the TJ complex in the pathogenesis of brain edema in FHF has not been explored. We thus hypothesized that altered TJ proteins lead to increased BBB permeability resulting in brain edema in FHF. The purpose of this study was to examine TJ composition in a well-characterized murine model of FHF [12-14]. We examined protein expression and cellular distribution for occludin, claudin-5, ZO-1, and ZO-2 in microvessels isolated from brains of normal control and FHF-induced mice.

METHODS

Animals

Male C57BL/6J mice (Jackson Laboratory, Bar Harbor, ME), 10-14 weeks old, were housed in a conventional mouse room with 12-h light/dark cycles and food and water ad libitum. The protocol for experimental use of animals was approved by the Mayo Clinic in accordance with The National Institutes of Health Guide for the Care and Use of Laboratory Animals.

Fulminant Hepatic Failure Model

FHF was induced by azoxymethane (AOM; Sigma, St. Louis, MO) as previously described [12]. The progression of hepatic encephalopathy was determined clinically, as follows: stage I, decreased movements; stage II, gait ataxia and lethargy; stage III, coma with righting and extremity reflexes present; stage IV, comatose with loss of righting reflexes. We refer to stages I and II as precoma, and stages III and IV as comatose. Serum alanine aminotransferase (ALT) and liver histology were analyzed to confirm the liver damage. BBB permeability was assessed by measuring sodium fluorescein extravasation.

Experimental Protocol

In each experiment, the study animals were divided into the following three groups: control, precoma, and comatose. Mice in the precoma and comatose groups received a single intraperitoneal injection of AOM (50 $\mu\text{g/g}$) dissolved in saline at 10 $\mu\text{L/g}$ of body weight and were sacrificed at either the precoma or the comatose hepatic encephalopathy stage. Control mice received an equivalent volume of saline. Twenty mice were assigned to each experiment, and the experiment was repeated four times.

After injection of AOM, behavior and body temperature were monitored. Heating pads were used to prevent hypothermia. Body temperature was monitored using a rectal probe. To avoid dehydration, hypoglycemia, and acidosis, a supplement solution of 1.68% sodium bicarbonate and 10% dextrose in 0.225% normal saline was given (1.0 mL/mouse) at 12 and 20 h after AOM injection, then 0.5 mL/mouse was given every 2 h after encephalopathy progressed to stage II.

Liver Function Test

When mice were sacrificed, blood was drawn immediately from the right atrium to obtain serum. ALT level was measured by a colorimetric kit (BioTron Diagnostics Co., Hemet, CA).

Liver Histology

Liver samples were fixed in 10% paraformaldehyde and embedded in paraffin. Sections (5 μm) were stained with hematoxylin and eosin (H&E) and examined by light microscopy.

Blood-Brain Barrier Permeability

Sodium fluorescein (molecular weight, 376 Da) was used to assess the BBB permeability as previously described [15], in a manner similar to the previous use of Evans blue dye [12]. Mice received an intravenous injection of 8 mL/kg of 0.6% sodium fluorescein at each designated hepatic encephalopathy stage. For precoma FHF mice, sodium fluorescein was given in the middle of stage II. For comatose FHF mice, sodium fluorescein was given at the end of stage III. For normal control and precoma groups, pentobarbital (40 mg/kg) was given as anesthesia prior to sodium fluorescein injection. Thirty minutes later, mice were perfused with 10 mL of normal saline. Brains were resected and brain stems removed. A hemisphere of cerebrum was homogenized in 30% trichloroacetic acid followed by centrifugation at $10,000 \times g$ for 5 min. From the supernatant, sodium fluorescein concentration was measured with a fluorometer at 460 nm as excitation wavelength and at 515 nm as emission wavelength.

Microvessel Isolation

Brain microvessels were isolated for Western blot and immunofluorescent microscopy (IFM) according to previous reports, with some modifications [16]. Brains were obtained at each designated hepatic encephalopathy stage. For precoma FHF mice, brains were resected in the middle of stage II. For comatose mice, brains were resected immediately upon the loss of corneal reflexes. Resected brains were cleared from the pia mater and brain stems removed. Minced brain samples were homogenized in 1.25 mL of ice-cold PBS-GS buffer (0.45% glucose and 3% sucrose in PBS, pH 7.35 ± 0.05 , 340 ± 5 mOsm) for 20 strokes. Homogenates were passed through 180- μm nylon mesh (Millipore, Bedford, MA) with a Swinnex filter holder (Millipore). The filtrates were centrifuged at $100 \times g$ for 10 min at 4°C . The pellet was resuspended in 2.5 mL of PBSGS and passed through 60- μm nylon mesh (Millipore). The samples attached to the mesh were washed five times, each with 2.5 mL of PBS-GS, and the remaining material on the mesh consisted of isolated microvessels. The quality of the microvessel fractions was checked by H&E staining and confirmed with electron microscopy.

Protein Extraction

Isolated microvessels were extracted with buffer containing 20 mM Tris-HCl (pH 7.5), 150 mM NaCl, 0.5% Triton X-100, 0.5% NP-40, 2 mM CaCl₂, 1 mM Na orthovanadate, phosphatase inhibitor cocktail 2 (Sigma P 5726), 1 mL/100 mL extraction buffer, protease inhibitor cocktail (Sigma P 8340), 1 mL/100 mL extraction buffer, and 1 mM PMSF, similar to that used in a previous study [15]. Proteins were extracted into two different fractions as previously described [17,18]. Homogenates were centrifuged at 3300 × *g* for 10 min at 4°C, and supernatant was collected as Triton-NP40-soluble proteins. The pellet was lysed in 1% or 4% SDS. Homogenates were centrifuged at 3300 × *g* for 10 min at 4°C and supernatant collected as SDS-soluble proteins. The total protein concentration of the microvessel extracts was measured by the bicinchoninic acid (BCA) protein assay (Pierce, Rockford, IL).

Western Blot Assay

The assay was performed as previously described [5]. Protein isolated from microvessels was analyzed for expression of the TJ proteins occludin, claudin-5, ZO-1 and ZO-2, and the endothelial cell marker caveolin. Microvessel protein samples (30 μg in Triton-soluble fraction and 15 μg in SDS-soluble fraction) were mixed with 4× Nu PAGE LDS sample buffer (Invitrogen, Carlsbad, CA) in reducing conditions and boiled for 3 min before loading. Proteins were separated by sodium dodecyl sulfate (SDS)-polyacrylamide gel electrophoresis (4%-20% Tris-HCl, gradient gels; Bio-Rad, Hercules, CA) and transferred electronically to polyvinylidene difluoride membranes (Millipore). The membranes were blocked with 5% nonfat milk in PBS containing 0.1% Tween 20 (PBS-T) for 1 h and then with primary antibodies to occludin, ZO-2, and caveolin (BD Bioscience, San Jose, CA) and claudin-5 and ZO-1 (Zymed Laboratories Inc., South San Francisco, CA) for 1 h at room temperature or overnight at 4°C. All the antibodies for occludin, claudin-5, and ZO-2 were monoclonal, and antibodies for ZO-1 and caveolin were polyclonal. After six washings with PBS-T, the membranes were incubated for 1 h at room temperature with HRP-conjugated secondary antibodies to goat anti-mouse IgG (SouthernBiotech, Birmingham, AL) or goat anti-rabbit IgG (Southern-Biotech). After washing membranes six times in PBS-T, protein expression was visualized by enhanced chemiluminescence reagent (Amersham Biosciences, Piscataway, NJ) and exposure to Hyperfilm (Amersham Biosciences). Bands were quantified using ImageQuant software (Molecular Dynamics, Sunnyvale, CA).

Immunofluorescent Microscopy

Immunofluorescent microscopy (IF) was performed as previously described [19]. The isolated microvessels were smeared onto microscope slides, air dried for 2-8 h, fixed with methanol for 2 min, and incubated with 1.5% goat normal serum for 30 min in PBS. Slides were incubated with primary antibodies to occludin, claudin-5, and ZO-1 (Zymed Laboratories Inc.), and ZO-2 and caveolin (BD Bioscience) in PBS with 1.5% goat normal serum for 1 h at room temperature. After being rinsed, slides were incubated with Alexa Fluor 488-conjugated anti-mouse or anti-rabbit IgG (Invitrogen) and diluted in 1.5% goat normal serum in PBS for 30 min. Microvessels from normal control, precoma, and comatose animals were stained simultaneously for each antigen. The slides were sealed with coverslips and Vectashield (Vector Laboratories, Burlingame, CA). Images were taken with 100× oil-immersion objectives on an Olympus BX50 fluorescence microscope (Olympus Optical, Tokyo, Japan) with a fluorescein filter.

Statistical Analysis

Results are expressed as mean ± SEM. Statistical comparisons were performed using ANOVA followed by two-sample *t*-test with a Bonferroni adjustment. A *p* value less than .05 was considered statistically significant.

RESULTS

Fulminant Hepatic Failure in Mice

Control mice without AOM remained normal. After a single injection of AOM, FHF mice displayed a reproducible progression to stages I and II of encephalopathy (precoma) within 23.1 h and to stages III and IV (coma) by 26.3 h. Liver damage was confirmed by elevated serum ALT (control, 12 ± 3 ; precoma, $12,404 \pm 306$; coma, $13,161 \pm 484$ IU/L), which correlated with the histology of hepatocellular necrosis (data not shown). These results were consistent previous findings by us and others [12-14].

Body temperatures of control and FHF mice were monitored. Although the FHF mice were maintained continuously on heated beddings, they still had mild hypothermia, $34.2 \pm 0.5^\circ\text{C}$, compared with normothermia, $37.4 \pm 0.1^\circ\text{C}$, in the normal control mice. These findings were consistent with a previous report [20].

Increased BBB Permeability in FHF Mice

BBB permeability was determined using sodium fluorescein. In control and precoma FHF mice, we found a similar level of sodium fluorescein extravasation in brain tissue. In contrast, comatose FHF mice had a twofold higher level of sodium fluorescein extravasation than control and precoma mice (Figure 1), demonstrating increased BBB permeability. These results were consistent with our previous findings and those of others [12,21,22].

Isolated Microvessels

Microvessels were isolated from brains of normal control, precoma, and comatose FHF mice. The preparations consisted mainly of microvessels without astrocytes as determined by histological examination of H&E stainings. Using this technique we established that the purity of the preparations was greater than 90% (Figure 2). Most of the microvessels were smaller than $10 \mu\text{m}$, consistent with the size of capillaries. Although not shown, electron microscopy was used to confirm the presence of microvessels without astrocytes in the preparations.

Decreased Expression of ZO-2 in Brain Microvessels of FHF Mice

To examine the expression of TJ proteins (occludin, claudin-5, ZO-1, and ZO-2), Western blot was performed with equal amounts of protein from each sample. Caveolin served as the specific cellular surface marker of endothelial cells. Each microvessel preparation was divided into Triton-NP40-soluble and SDS-soluble fractions.

When we examined the SDS-soluble fraction, ZO-2 was significantly lower in brains of precoma and comatose FHF mice (Figure 3). The precoma and comatose FHF mice had significantly less ZO-2 ($76.6 \pm 6.6\%$ [$n = 9$] and $78.9 \pm 4.8\%$ [$n = 14$]), respectively, compared with 100.0% in control mice ($n = 9$; $p < .05$). However, we found no differences in the expression of TJ proteins in the Triton-NP40-soluble fraction in precoma and comatose FHF mice compared with control animals (data not shown).

As seen in Figure 3, the caveolin level was the same in all samples from all groups of mice. These findings indicate equivalent amounts of microvessel endothelial cells and consistency in the purity of the preparations. This is in agreement with findings of another laboratory, in which caveolin level remains unchanged during FHF [23].

Altered Distribution of ZO-2 in Brain Microvessels of FHF Mice

We investigated the cellular distribution of TJ proteins by using IF. In control animals, occludin, ZO-1, and ZO-2 showed a continuous linear staining pattern along the presumed

regions of TJ between endothelial cells in the isolated microvessels (Figures 4A, 4G, and 4J). Claudin-5 had a punctate staining pattern that was evenly scattered along the cells of the isolated microvessels (Figure 4D). There were no alterations in IF intensity or distribution patterns for occludin, claudin-5, and ZO-1 in microvessels isolated from precoma mice (Figures 4B, 4E, and 4H) or comatose FHF mice (Figures 4C, 4F, and 4I) compared with control animals (Figures 4A, 4D, and 4G). In contrast, ZO-2 showed distinct perturbations in IF pattern in microvessels of FHF mice. In precoma FHF mice, ZO-2 staining showed disruptions-including clumps or particles (Figure 4K)-compared with the continuous linear pattern in control mice. These alterations in ZO-2 distribution became more evident in microvessels of comatose FHF mice (Figure 4L).

Caveolin exhibited a diffuse pattern of IF staining in microvessels from animals in all three study groups (Figures 4M, 4N, and 4O), suggesting that caveolin was not affected by FHF. This is consistent with previous findings [23].

No signal was seen in the absence of a primary antibody (data not shown).

DISCUSSION

The role of the TJ complex in the pathogenesis of brain edema in FHF is poorly understood. In this study, we found a significant and specific perturbation in the TJ protein ZO-2 in association with increased BBB permeability in a murine model of FHF. The changes in ZO-2 distribution occurred in the precoma stages, although no increase in BBB permeability occurred then. The ZO-2 changes became more prominent in the comatose stages of FHF, at the beginning of which a significant increase in BBB permeability was observed. The perturbation in ZO-2 composition thus preceded the onset of the increased BBB permeability.

Normal function of the BBB requires the integrity of the endothelial cellular TJ complex. The ZO family consists of ZO-1, -2, and -3, and they are members of the membrane-associated guanylate kinase homologous family, with a COOH terminal binding to the claudins [24]. They also link other transmembrane TJ proteins, including occludin and the actin cytoskeleton in endothelial cells [25]. It has been shown that ZO-1 and ZO-2 can affect claudin independently [26].

Alterations in TJ composition are known to lead to compromised BBB function. For example, in an in vivo murine model of transient focal cerebral ischemia, ZO-1 was significantly decreased, correlating with increased BBB permeability [5]. In a rat model of microsphere-induced cerebral embolism with increased BBB leakage, Kago et al. found significantly lower levels of occludin and ZO-1 and greater tyrosine phosphorylation of occludin in isolated brain microvessels [6]. TJ proteins have also been examined using in vitro models of BBB. Hypoxia-reoxygenation, hydrogen peroxide, and other oxidants were shown to alter occludin, ZO-1, and ZO-2 in brain-derived microvascular endothelial cells [17,27,28]. BBB permeability is regulated by monocyte chemoattractant protein-1, which changes the cellular distribution of these TJ proteins [29]. Altered TJ protein composition was shown to correlate with BBB permeability found in decompensated hemorrhagic shock [15]. Recently, decreased expression of ZO-2 but not occludin, claudin-5, or ZO-1 was demonstrated in spontaneously hypertensive rats, a well-known model of increased susceptibility to cerebral ischemia [30]. Collectively, these findings suggest that even subtle alterations in TJ composition can result in BBB dysfunction.

In the present study, we observed altered TJ composition only in ZO-2. From other reports, occludin and ZO-1 are the likely targets for matrix metalloproteinase (MMP)-9 influence, as seen in brain ischemia [5] and diabetic retinopathy [31]. However, minor alterations in these TJ proteins can be obscured while isolating brain microvessels and might not be readily

detected. In addition, when FHF mice were treated with the MMP-9 mAb, ZO-2 was not restored (data not shown). These findings suggest that ZO-2 might be involved in MMP-independent pathways that are directly or indirectly related to BBB permeability. One such mechanism is MMP-independent phosphorylation of TJ components of BBB [32]. It has been shown that BBB permeability might be regulated and modulated by the phosphorylation of TJ elements [33,34]. For example, tyrosine phosphorylation of occludin diminishes its interactions with ZO-1, ZO-2, and ZO-3 [35]. Indeed, ZO-2 is a target of phosphorylation by protein kinase C [36]. Further investigations of the mechanism by which ZO-2 is altered are warranted.

In conclusion, we found a significant and specific perturbation in the tight junction ZO-2 that precedes the increased BBB permeability in FHF mice. These findings suggest a potential specific role of ZO-2 in the integrity of the BBB in FHF.

Acknowledgements

The work in this paper was supported by NIH DK064361, NIH R01NS051646, AHA 0655589B; and Deason Foundation. We wish to thank Monica Castanedes-Casey and Dr. Justus Daechsel for their technical assistance and Lisa Moroski for her editorial assistance.

REFERENCES

- [1]. Vaquero J, Blei AT. Etiology and management of fulminant hepatic failure. *Curr Gastroenterol Rep* 2003;5:39–47. [PubMed: 12530947]
- [2]. Larsen FS, Wendon J. Brain edema in liver failure: basic physiologic principles and management. *Liver Transpl* 2002;8:983–989. [PubMed: 12424710]
- [3]. Ede RJ, Williams RW. Hepatic encephalopathy and cerebral edema. *Semin Liver Dis* 1986;6:107–118. [PubMed: 3018935]
- [4]. Harhaj NS, Antonetti DA. Regulation of tight junctions and loss of barrier function in pathophysiology. *Int J Biochem Cell Biol* 2004;36:1206–1237. [PubMed: 15109567]
- [5]. Asahi M, Wang X, Mori T, et al. Effects of matrix metalloproteinase-9 gene knock-out on the proteolysis of blood-brain barrier and white matter components after cerebral ischemia. *J Neurosci* 2001;21:7724–7732. [PubMed: 11567062]
- [6]. Kago T, Takagi N, Date I, et al. Cerebral ischemia enhances tyrosine phosphorylation of occludin in brain capillaries. *Biochem Biophys Res Commun* 2006;339:1197–1203. [PubMed: 16338221]
- [7]. Wolburg H, Lippoldt A. Tight junctions of the blood-brain barrier: development, composition and regulation. *Vascul Pharmacol* 2002;38:323–337. [PubMed: 12529927]
- [8]. Wolburg H, Wolburg-Buchholz K, Kraus J, et al. Localization of claudin-3 in tight junctions of the blood-brain barrier is selectively lost during experimental autoimmune encephalomyelitis and human glioblastoma multiforme. *Acta Neuropathol (Berl)* 2003;105:586–592. [PubMed: 12734665]
- [9]. Nitta T, Hata M, Gotoh S, et al. Size-selective loosening of the blood-brain barrier in claudin-5-deficient mice. *J Cell Biol* 2003;161:653–660. [PubMed: 12743111]
- [10]. Desjardins P, Belanger M, Butterworth RF. Alterations in expression of genes coding for key astrocytic proteins in acute liver failure. *J Neurosci Res* 2001;66:967–971. [PubMed: 11746425]
- [11]. Belanger M, Desjardins P, Chatauret N, et al. Selectively increased expression of the astrocytic/endothelial glucose transporter protein GLUT1 in acute liver failure. *Glia* 2006;53:557–562. [PubMed: 16374780]
- [12]. Nguyen JH, Yamamoto S, Steers J, et al. Matrix metalloproteinase-9 contributes to brain extravasation and edema in fulminant hepatic failure mice. *J Hepatol* 2006;44:1105–1114. [PubMed: 16458990]
- [13]. Matkowskyj KA, Marrero JA, Carroll RE, et al. Azoxymethane-induced fulminant hepatic failure in C57BL/6J mice: characterization of a new animal model. *Am J Physiol* 1999;277:G455–G462. [PubMed: 10444460]

- [14]. Belanger M, Cote J, Butterworth RF. Neurobiological characterization of an azoxymethane mouse model of acute liver failure. *Neurochem Int* 2006;48:434–440. [PubMed: 16563565]
- [15]. Krizbai IA, Lenzser G, Szatmari E, et al. Blood-brain barrier changes during compensated and decompensated hemorrhagic shock. *Shock* 2005;24:428–433. [PubMed: 16247328]
- [16]. Grammas P. A damaged microcirculation contributes to neuronal cell death in Alzheimer's disease. *Neurobiol Aging* 2000;21:199–205. [PubMed: 10867204]
- [17]. Musch MW, Walsh-Reitz MM, Chang EB. Roles of ZO-1, occludin, and actin in oxidant-induced barrier disruption. *Am J Physiol Gastrointest Liver Physiol* 2006;290:G222–G231. [PubMed: 16239402]
- [18]. Pflugfelder SC, Farley W, Luo L, et al. Matrix metalloproteinase-9 knockout confers resistance to corneal epithelial barrier disruption in experimental dry eye. *Am J Pathol* 2005;166:61–71. [PubMed: 15632000]
- [19]. Hawkins BT, Abbruscato TJ, Egleton RD, et al. Nicotine increases in vivo blood-brain barrier permeability and alters cerebral microvascular tight junction protein distribution. *Brain Res* 2004;1027:48–58. [PubMed: 15494156]
- [20]. Traber P, DalCanto M, Ganger D, et al. Effect of body temperature on brain edema and encephalopathy in the rat after hepatic devascularization. *Gastroenterology* 1989;96:885–891. [PubMed: 2914649]
- [21]. Dixit V, Chang TM. Brain edema and the blood brain barrier in galactosamine-induced fulminant hepatic failure rats. An animal model for evaluation of liver support systems. *ASAIO Trans* 1990;36:21–27. [PubMed: 2306387]
- [22]. Livingstone AS, Potvin M, Goresky CA, et al. Changes in the blood-brain barrier in hepatic coma after hepatectomy in the rat. *Gastroenterology* 1977;73:697–704. [PubMed: 892373]
- [23]. Sawara K, Desjardins P, Jian W, et al. Temperature-sensitive alterations in expression of vascular endothelial genes in brains of rats with acute liver failure. *Hepatology* 2006;44(Suppl 1):479A.
- [24]. Itoh M, Furuse M, Morita K, et al. Direct binding of three tight junction-associated MAGUKs, ZO-1, ZO-2, and ZO-3, with the COOH termini of claudins. *J Cell Biol* 1999;147:1351–1363. [PubMed: 10601346]
- [25]. Wittchen ES, Haskins J, Stevenson BR. Protein interactions at the tight junction. Actin has multiple binding partners, and ZO-1 forms independent complexes with ZO-2 and ZO-3. *J Biol Chem* 1999;274:35179–35185. [PubMed: 10575001]
- [26]. Umeda K, Ikenouchi J, Katahira-Tayama S, et al. ZO-1 and ZO-2 independently determine where claudins are polymerized in tight-junction strand formation. *Cell* 2006;126:741–754. [PubMed: 16923393]
- [27]. Mark KS, Davis TP. Cerebral microvascular changes in permeability and tight junctions induced by hypoxia-reoxygenation. *Am J Physiol Heart Circ Physiol* 2002;282:H1485–H1494. [PubMed: 11893586]
- [28]. Fischer S, Wiesnet M, Renz D, et al. H₂O₂ induces paracellular permeability of porcine brain-derived microvascular endothelial cells by activation of the p44/42 MAP kinase pathway. *Eur J Cell Biol* 2005;84:687–697. [PubMed: 16106912]
- [29]. Stamatovic SM, Shakui P, Keep RF, et al. Monocyte chemoattractant protein-1 regulation of blood-brain barrier permeability. *J Cereb Blood Flow Metab* 2005;25:593–606. [PubMed: 15689955]
- [30]. Hom S, Fleegal MA, Egleton RD, et al. Comparative changes in the blood-brain barrier and cerebral infarction of SHR and WKY rats. *Am J Physiol Regul Integr Comp Physiol* 2007;292:R1881–892. [PubMed: 17234953]
- [31]. Hawkins BT, Lundeen TF, Norwood KM, et al. Increased blood-brain barrier permeability and altered tight junctions in experimental diabetes in the rat: contribution of hyperglycaemia and matrix metalloproteinases. *Diabetologia* 2007;50:202–211. [PubMed: 17143608]
- [32]. Lohmann C, Krischke M, Wegener J, et al. Tyrosine phosphatase inhibition induces loss of blood-brain barrier integrity by matrix metalloproteinase-dependent and -independent pathways. *Brain Res* 2004;995:184–196. [PubMed: 14672808]
- [33]. Branton JL, Wong V, Wang W, et al. Reduction of tyrosine kinase activity and protein tyrosine dephosphorylation by anoxic stimulation in vitro. *Neuroscience* 1998;82:161–70. [PubMed: 9483512]

- [34]. Staddon J, Ratcliffe M, Morgan L, et al. Protein phosphorylation and the regulation of cell-cell junctions in brain endothelial cells. *Heart Vessels* 1997;(suppl 12):106–109. [PubMed: 9476557]
- [35]. Kale G, Naren AP, Sheth P, et al. Tyrosine phosphorylation of occludin attenuates its interactions with ZO-1, ZO-2, and ZO-3. *Biochem Biophys Res Commun* 2003;302:324–329. [PubMed: 12604349]
- [36]. Avila-Flores A, Rendon-Huerta E, Moreno J, et al. Tight-junction protein zonula occludens 2 is a target of phosphorylation by protein kinase C. *Biochem J* 2001;360:295–304. [PubMed: 11716757]

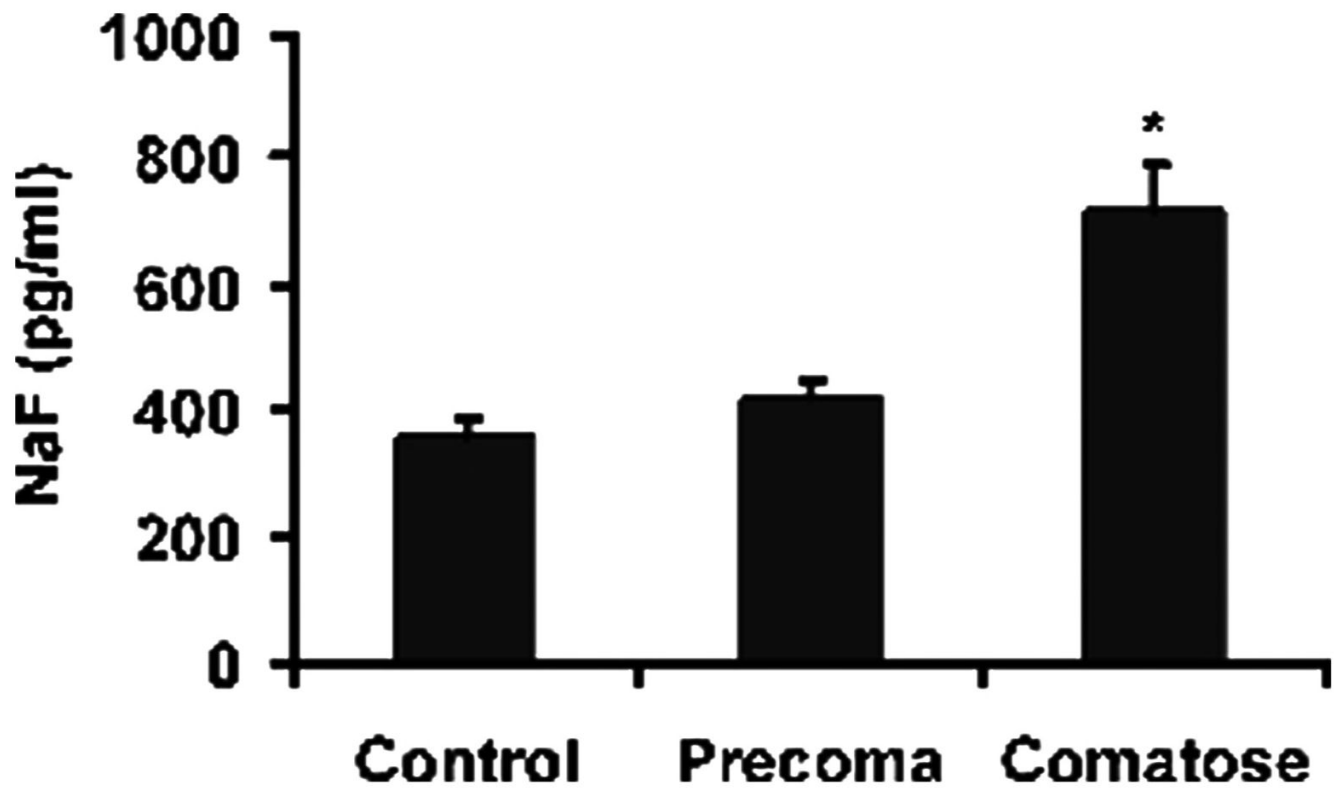


FIGURE 1.

Increased BBB permeability in comatose FHF mice. Brain extravasation of sodium fluorescein was determined in mice from the control, precoma, and comatose groups. The brains of comatose FHF mice had significantly greater sodium fluorescein extravasation ($*P < .01$) compared with control brains, whereas brains of precoma FHF mice showed no significant difference. $n = 5$ in each group.

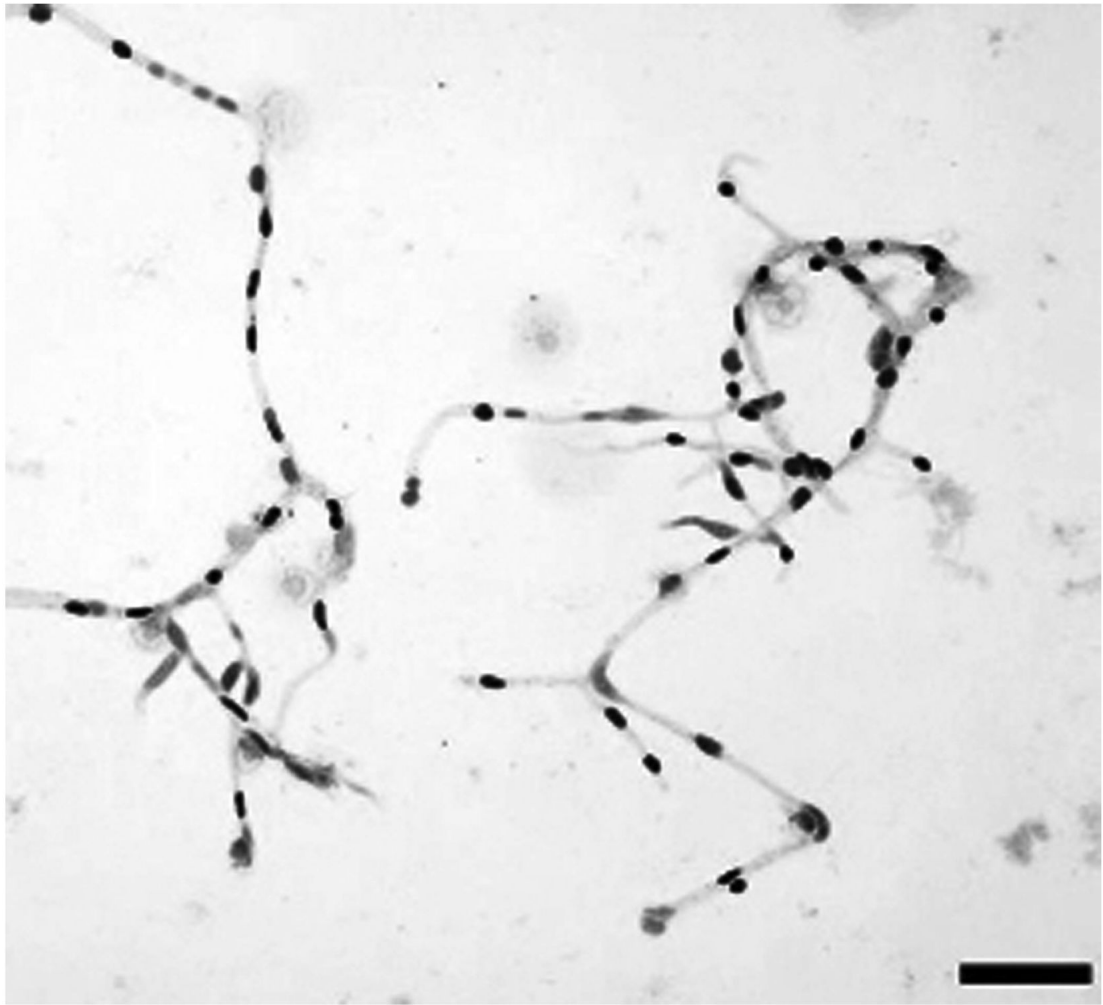
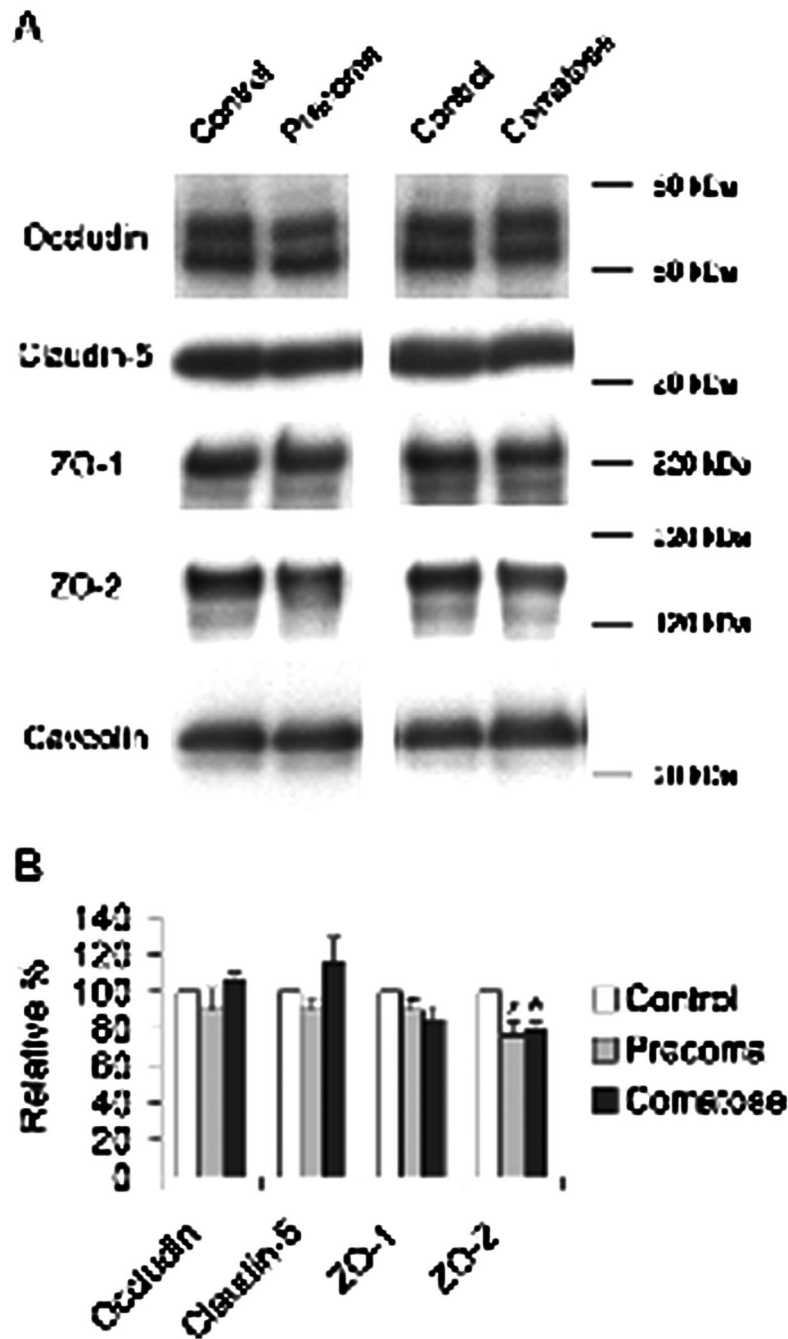


FIGURE 2. Isolated microvessels from brains of study mice. H&E staining; magnification, $\times 200$. Scale bar = $20 \mu\text{m}$.

**FIGURE 3.**

A: Western blots of occludin, claudin-5, ZO-1, and ZO-2 in the SDS-soluble fraction of isolated brain microvessels. Caveolin was used as an endothelial specific marker. B: Densitometric analysis of each TJ protein. Each TJ protein was expressed as a ratio against caveolin. ZO-2 was $76.6\% \pm 6.6\%$ in precoma FHF and $78.9\% \pm 4.8\%$ in comatose FHF mice compared with ZO-2 level in control mice (100%) (* $P < .05$). $n = 9$ in control and precoma FHF groups, $n = 14$ in comatose FHF group for all antigens except ZO-1 for which $n = 4$ in each group.

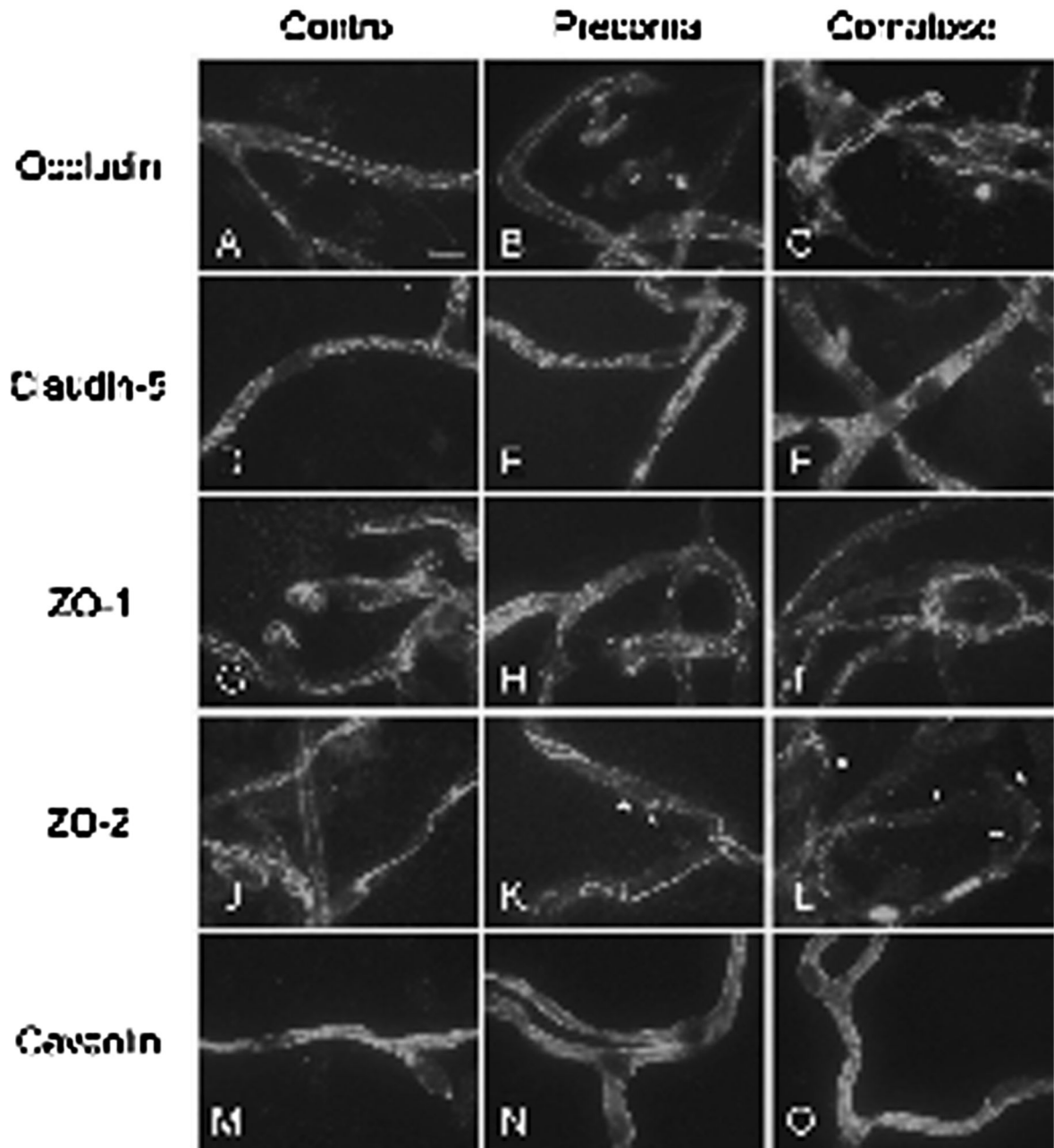


FIGURE 4.

Immunofluorescent localization of TJ proteins in isolated cerebral microvessels. A-C: occludin; D-F: claudin-5; G-I: ZO-1; and J-L: ZO-2. Caveolin served as an endothelial specific marker (M-O). ZO-2 formed clumps or particles in the microvessels of the precoma FHF mice (asterisk). The particles became more evident in the comatose FHF group. Scale bar = 10 μ m.